

Spin Hall and spin Nernst effect in dilute ternary alloys

Katarina Tauber,^{1,*} Dmitry V. Fedorov,¹ Martin Gradhand,² and Ingrid Mertig^{1,3}

¹Max Planck Institute of Microstructure Physics, Weinberg 2, 06120 Halle, Germany

²H. H. Wills Physics Laboratory, University of Bristol, Bristol BS8 1TL, United Kingdom

³Institute of Physics, Martin Luther University Halle-Wittenberg, 06099 Halle, Germany

(Received 7 February 2013; published 19 April 2013)

We report on *ab initio* studies of the spin Hall and spin Nernst effect in dilute ternary alloys. Our calculations are performed for a Cu host with different types of substitutional impurities. The obtained numerical results are well approximated by Matthiessen's rule relying on the constituent binary alloys. We show that the spin Nernst effect can be significantly more efficient in a ternary alloy with respect to the related binary alloys. Together with the application of Matthiessen's rule this opens an easy way to design materials for spintronics applications.

DOI: [10.1103/PhysRevB.87.161114](https://doi.org/10.1103/PhysRevB.87.161114)

PACS number(s): 72.25.Ba, 71.15.Rf, 72.15.Jf, 85.75.—d

The spin Hall effect (SHE), which was predicted by Dyakonov and Perel in 1971,¹ is one of the most promising research topics in the field of spintronics. It describes the separation of electrons with antiparallel spins lateral to an electrical current.² The direct experimental verification was provided 33 years later by Kato *et al.*,³ who observed the spin accumulation optically via Kerr rotation. However, an indirect measurement of the SHE was performed by Fert *et al.*⁴ much earlier via studies of the anomalous Hall effect (AHE) in ternary alloys. Nowadays, the inverse SHE offers a simple method to detect a spin current via its conversion into a charge current.⁵ The importance of the SHE for practical applications arises from the advantage to generate spin currents in nonmagnetic materials without spin injection from ferromagnets. Normally, three main contributions to the SHE, as well as for the AHE,⁶ are discussed in literature. Namely, they are the intrinsic contribution due to the anomalous velocity^{7,8} and the extrinsic skew-scattering^{9,10} and side-jump¹¹ mechanisms. In dilute alloys the skew-scattering contribution is dominating.^{12–14} In that limit the spin Hall conductivity depends strongly on the impurity type, which can even cause a sign change of the spin Hall current in one and the same host crystal.^{15,16} Recently, a related phenomenon, the spin Nernst effect (SNE), was studied theoretically.^{17–22} This phenomenon is connected to the rapidly emerging field of *spin caloritronics*.^{23,24} The SNE describes the creation of a transverse spin current by an applied temperature gradient, in contrast to an electric field used for the SHE. The mechanisms contributing to the SNE are the same as introduced for the SHE.

Until now, the skew-scattering mechanism for both phenomena mentioned above was considered for binary alloys.^{12,15,16,20} In this Rapid Communication we present first-principles studies of the SHE and SNE in dilute Cu-based ternary alloys. Due to the long spin diffusion length, together with the strong SHE and SNE reachable by impurity tailoring,^{15,16,20,25,26} copper seems to be a good candidate for possible spintronic applications. Our work is motivated by the fact that in real systems more than one type of impurity can be present. Obviously, it is desirable to understand the influence of this to the considered phenomena. We will show that optimal combinations of different types of impurities in the same host material can enhance the generated spin current in comparison to the related binary alloys. Our investigated systems are Cu($A_{1-w}B_w$) alloys, where a Cu

host contains two different types of substitutional impurities labeled as A and B . In the considered dilute impurity limit, both charge and spin conductivity are inversely proportional to the impurity concentration.^{9,10,12–15} For our studies we fix the total concentration of impurities at 1 at. % to obtain comparable results. Thus, the quantity $w \in [0, 1]$ describes the weighting between the impurities A and B . It implies for $w = 0$ and $w = 1$ the system reduces to the binary alloys Cu(A) and Cu(B), respectively.

In our approach a fully relativistic Korringa-Kohn-Rostoker method²⁷ is used to obtain the electronic structure of the host and the impurity system. The transport properties are calculated within the semiclassical theory solving the linearized Boltzmann equation.^{15,28} In the considered dilute limit, the impurities are assumed to be noninteracting and consequently the scattering cross sections can be added. Therefore, the microscopic transition probability of the ternary alloy Cu($A_{1-w}B_w$) can be expressed by those of the related binary alloys Cu(A) and Cu(B) as²⁹

$$P_{kk'}^{ss'AB}(w) = (1 - w)P_{kk'}^{ss'A} + wP_{kk'}^{ss'B}. \quad (1)$$

Here, $P_{kk'}^{ss'}$ describes the scattering probability from an initial state $\{\mathbf{k}, s\}$ to a final state $\{\mathbf{k}', s'\}$, where for each crystal momentum \mathbf{k} there are two degenerate relativistic spin states labeled as $s = +$ and $s = -$.^{15,27} After solving the Boltzmann equation considering the corresponding spin-dependent microscopic transition probability, a conductivity tensor for each spin direction is calculated.¹⁵

Within the two-current model, which is employed for our calculations, the charge conductivity $\hat{\sigma}$ and the spin conductivity $\hat{\sigma}^s$ are represented by

$$\hat{\sigma} = \hat{\sigma}^+ + \hat{\sigma}^-, \quad \hat{\sigma}^s = \hat{\sigma}^+ - \hat{\sigma}^-. \quad (2)$$

This is a good approximation for a Cu host, where the electron spin polarization, expressed in units of $\hbar/2$, is higher than 0.99.²⁷ The results of our calculations presented below are obtained neglecting spin-flip transitions for the SNE but including them for the SHE, following to the corresponding approaches of Refs. 20 and 15.

For a nonmagnetic cubic host with z as the global quantization axis, the spin-dependent conductivity tensors are

given by

$$\hat{\sigma}^+ = \begin{pmatrix} \sigma_{xx}^+ & -\sigma_{yx}^+ & 0 \\ \sigma_{yx}^+ & \sigma_{xx}^+ & 0 \\ 0 & 0 & \sigma_{zz}^+ \end{pmatrix} = (\hat{\sigma}^-)^T, \quad (3)$$

where the superscript T denotes the transpose. The resistivity tensors $\hat{\rho}^\pm = (\hat{\sigma}^\pm)^{-1}$ have similar structures. One can easily obtain

$$\rho_{xx}^+ = \frac{\sigma_{xx}^+}{(\sigma_{xx}^+)^2 + (\sigma_{yx}^+)^2}, \quad \rho_{yx}^+ = -\frac{\sigma_{yx}^+}{(\sigma_{xx}^+)^2 + (\sigma_{yx}^+)^2}, \quad (4)$$

where we have written only the components important for the further discussion. The relation between $\hat{\sigma}^+$ and $\hat{\sigma}^-$ in Eq. (3) is valid due to the time and space inversion symmetry of the considered systems. Consequently, it is sufficient to describe the longitudinal conductivity $\sigma_{xx} = 2\sigma_{xx}^+$ and the spin Hall conductivity $\sigma_{yx}^s = 2\sigma_{yx}^+$ in terms of one spin channel. The ratio of these quantities defines the spin Hall angle (SHA)

$$\alpha = \frac{\sigma_{yx}^s}{\sigma_{xx}} = \frac{\sigma_{yx}^+}{\sigma_{xx}^+} = -\frac{\rho_{yx}^+}{\rho_{xx}^+}, \quad (5)$$

which describes the efficiency of charge into spin current conversion.

The transport properties of a ternary alloy can be obtained either by a full calculation based on Eq. (1) and the formalism of Ref. 15 or by the approximation of Matthiessen's rule applied for each spin channel separately,^{29,30}

$$\hat{\rho}^{+AB} \equiv \hat{\rho}^{+AB}(w) = (1-w)\hat{\rho}^{+A} + w\hat{\rho}^{+B}. \quad (6)$$

Here, $\hat{\rho}^{+AB}$ is the resistivity tensor of the ternary alloy $\text{Cu}(A_{1-w}B_w)$. The resistivity tensors of the related binary alloys are $\hat{\rho}^{+A} = (\hat{\sigma}^{+A})^{-1}$ and $\hat{\rho}^{+B} = (\hat{\sigma}^{+B})^{-1}$. The inversion yields

$$\begin{aligned} \sigma_{xx}^{AB} &= \frac{2\rho_{xx}^{+AB}}{(\rho_{xx}^{+AB})^2 + (\rho_{yx}^{+AB})^2}, \\ \sigma_{yx}^{sAB} &= -\frac{2\rho_{yx}^{+AB}}{(\rho_{xx}^{+AB})^2 + (\rho_{yx}^{+AB})^2} \end{aligned} \quad (7)$$

for the longitudinal conductivity and the spin Hall conductivity (SHC) of the considered ternary alloy.

As a first result, we present a comparison between the full calculation and the approximation by Matthiessen's rule. For this purpose alloys of the form $\text{Cu}(A_{0.5}B_{0.5})$ are chosen. In Fig. 1 the relative deviations of the full calculations from Matthiessen's rule,

$$\frac{\Delta\rho_{ij}}{\rho_{ij}} = \frac{\rho_{ij}^{+AB} - \frac{1}{2}(\rho_{ij}^{+A} + \rho_{ij}^{+B})}{\frac{1}{2}(\rho_{ij}^{+A} + \rho_{ij}^{+B})}, \quad (8)$$

are visualized for ρ_{xx}^{+AB} and ρ_{yx}^{+AB} . Obviously, for the considered alloys Matthiessen's rule gives a good approximation of the full calculation with maximal relative deviations less than 15%. The reason for this is the approximately spherical Fermi surface of copper, since for spherical bands Matthiessen's rule holds exactly.³⁰ For the longitudinal resistivity, the deviations are always positive,^{29,30} since ρ_{xx}^+ is mainly determined by the symmetric part, $(P_{kk}^{++} + P_{kk}^{+-})/2$,

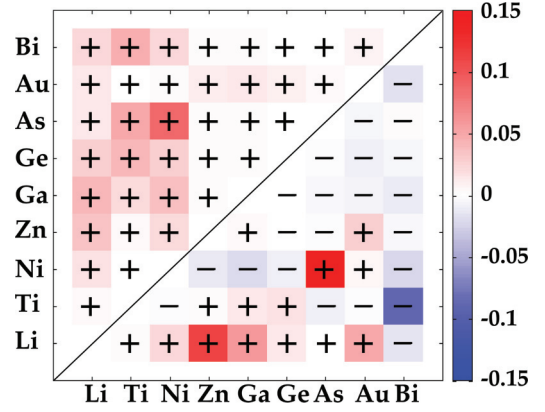


FIG. 1. (Color online) Relative deviations of the longitudinal and Hall resistivity, $\Delta\rho_{xx}/\rho_{xx}$ (upper left half) and $\Delta\rho_{yx}/\rho_{yx}$ (lower right half), respectively, for $\text{Cu}(A_{0.5}B_{0.5})$ alloys.

of the transition probability. By contrast, the Hall resistivity ρ_{yx}^+ is caused by the antisymmetric part, $(P_{kk}^{+-} - P_{kk}^{++})/2$.³¹ Consequently, $\Delta\rho_{yx}/\rho_{yx}$ is not restricted to be positive.

Now, let us consider the results of our calculations in the whole range of the weighting factor w for some selected alloys, which illustrate distinct characteristics. They are shown in Fig. 2 for the spin Hall and longitudinal conductivity given by Eq. (7) as well as for the spin Hall angle defined by Eq. (5). The lines are obtained applying Matthiessen's rule of Eq. (6), while the dots are results from the full calculations. For simplicity, the impurity labels A and B are chosen in a way that $\sigma_{xx}^A > \sigma_{xx}^B$. The behavior of the conductivities can be explained under the assumption $|\rho_{yx}^{+AB}| \ll \rho_{xx}^{+AB}$, which is valid for the considered systems. Then $\sigma_{xx}^{AB} \approx 2(\rho_{xx}^{+AB})^{-1}$ holds, where ρ_{xx}^{+AB} has a linear slope within Matthiessen's rule given by Eq. (6). Therefore, we obtain hyperbolae for the longitudinal conductivities, which are most pronounced if the ratio $\sigma_{xx}^A/\sigma_{xx}^B$ is high. The situation for the spin Hall conductivity is more interesting. As can be seen in Fig. 2, this quantity can have an extremum. Importantly, the absolute value of the extremum is not necessarily the largest value in the considered impurity regime. For instance, in the case of $\text{Cu}(\text{Zn}_{1-w}\text{Ti}_w)$ the maximal absolute value is present for the $\text{Cu}(\text{Zn})$ binary alloy. This originates from the opposite signs in the Hall conductivities for the corresponding binary alloys. Only for $\text{Cu}(\text{Au}_{1-w}\text{Bi}_w)$ an actual enhancement with respect to the constituent binary alloys is observed. Furthermore, an extremum occurs not in all cases. Within Matthiessen's rule and the assumption $|\rho_{yx}^{+AB}| \ll \rho_{xx}^{+AB}$, one can easily obtain an approximate position of the extremum,

$$w_E \approx \frac{\rho_{xx}^{+A}}{\rho_{xx}^{+B} - \rho_{xx}^{+A}} - \frac{2\rho_{yx}^{+A}}{\rho_{yx}^{+B} - \rho_{yx}^{+A}}, \quad (9)$$

for the SHC, which can be observed if $w_E \in [0, 1]$. Contrary to the SHC, the spin Hall angle shows no extremum. This follows, if we use Matthiessen's rule and analyze the first derivative of the spin Hall angle with respect to w . Indeed, with Eqs. (6) and (7) we obtain the condition for $\partial\alpha^{AB}/\partial w = 0$ as $\alpha^A \equiv -\rho_{yx}^{+A}/\rho_{xx}^{+A} = -\rho_{yx}^{+B}/\rho_{xx}^{+B} \equiv \alpha^B$. However, this is the

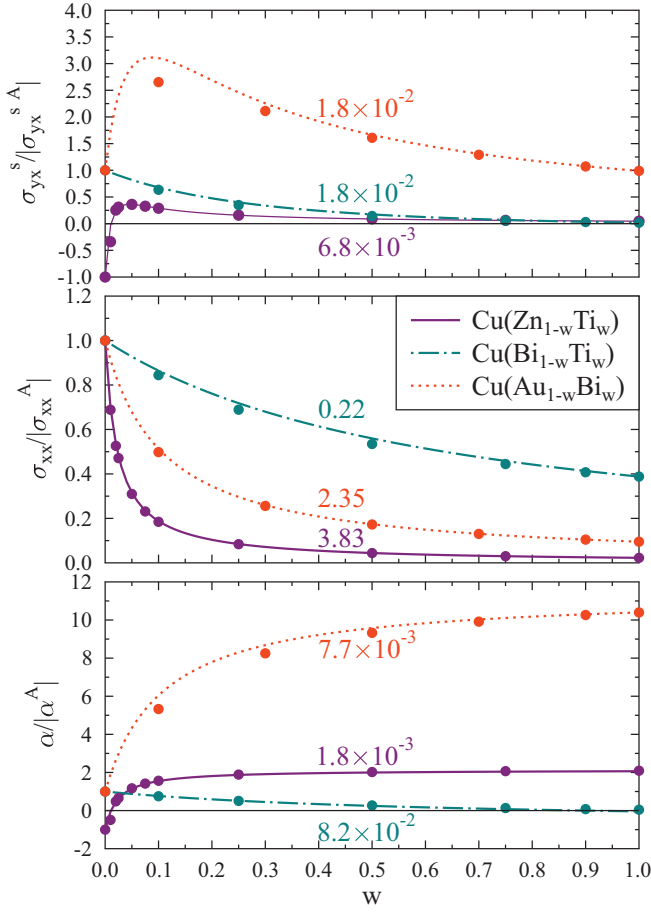


FIG. 2. (Color online) Spin Hall conductivity, longitudinal conductivity, and spin Hall angle for three $\text{Cu}(A_{1-w}B_w)$ alloys. An approximation via Matthiessen's rule (lines) and the values obtained with full calculations (dots) are shown. All curves are normalized to have the absolute values for $\text{Cu}(A)$ alloy equal to one. The multiplication of the curves with the scaling factors provides the actual values of the conductivities in units of $(\mu\Omega\text{cm})^{-1}$ and α (dimensionless).

trivial solution of a constant SHA for the ternary alloy. It implies that while the SHC can be enhanced for independent scatterers in a ternary alloy, α^{AB} is limited by the SHA of the constituent binary alloys.

Let us consider now the spin Nernst effect, which describes the creation of a spin current density j_y^s transverse to an applied temperature gradient $\nabla_x T$. Both quantities are connected by the spin Nernst conductivity (SNC) as $j_y^s = \sigma_{SN} \nabla_x T$.²⁰ To characterize the efficiency of the SNE, it is reasonable to use the ratio of j_y^s to the longitudinal heat current density $q_x = -\kappa \nabla_x T$, where κ is the heat conductivity.³² Within the formalism of Ref. 20 we obtain the efficiency of the SNE as

$$\gamma = \frac{\sigma_{SN}}{-\kappa} = \frac{\frac{2}{T} \left(\frac{L_{1,xx}^+}{L_{0,xx}^+} L_{0,yx}^+ - L_{1,yx}^+ \right)}{-\frac{2}{eT} \left(\frac{L_{1,xx}^+}{L_{0,xx}^+} - L_{2,xx}^+ \right)} \approx e \frac{\frac{L_{1,xx}^+}{L_{0,xx}^+} L_{0,yx}^+ - L_{1,yx}^+}{L_{2,xx}^+}, \quad (10)$$

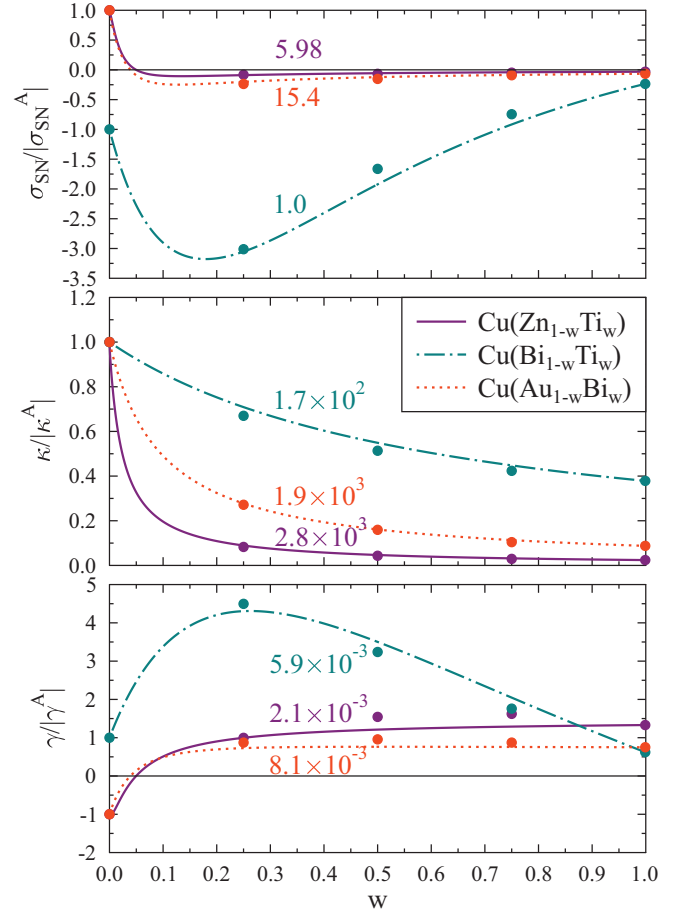


FIG. 3. (Color online) Spin Nernst conductivity, heat conductivity, and the ratio of both calculated via Matthiessen's rule (lines) and full calculations (dots) at 300 K. The given factors provide σ_{SN} in A/K m , κ in W/K m , and γ in $1/V$.

where $e = |e|$ is the elementary charge and the transport coefficients \hat{L}_n^+ are defined by²⁰

$$\hat{L}_n^+(T) = -\frac{1}{e} \int dE \hat{\sigma}^+(E) \left(-\frac{df_0(E,T)}{dE} \right) (E - \mu)^n. \quad (11)$$

The approximation in Eq. (10) is valid, since the term $(L_{1,xx}^+)^2 / L_{0,xx}^+$ is negligible for metals.³²

In Fig. 3 the SNC, the heat conductivity and the ratio of both is presented for the three ternary alloys. As was shown above, the SHC and the charge conductivity are well described by Matthiessen's rule. Consequently, this rule can be applied to approximate the transport coefficients of Eq. (11) for the ternary alloys. For this aim, we apply Matthiessen's rule given by Eq. (6) to an energy range around the Fermi level. Then, Eq. (7) yields the conductivities of the ternary alloys which are used to express the higher order moments of Eq. (11). The results shown in Fig. 3 approve the validity of this procedure. The SNC has an extremum for all the considered systems in contrast to the SHC. The curves for κ are hyperbolalike, similar to σ_{xx} in Fig. 2. This is a consequence of the Wiedemann-Franz law, which states the proportionality of charge and heat conductivity in metals. However, in contrast to the SHE, the efficiency of the SNE can have an extremum as shown in the lower panel of Fig. 3. Namely, for the $\text{Cu}(\text{Bi}_{1-w}\text{Ti}_w)$ alloy an

optimal weighting of the impurities can enhance γ by a factor of 4.5. Unfortunately, the extremum position cannot be easily expressed in terms of the transport properties of the binary alloys. All terms in Eq. (10) involve higher moments, which are strongly influenced by the actual energy dependence of the conductivities, according to Eq. (11). However, despite the lack of a simple analytic expression, pronounced extrema can be found graphically by applying our procedure based on Matthiessen's rule and using the known results for the constituent binary alloys.

In summary, we have studied the spin transport in dilute Cu-based ternary alloys transverse to applied electric fields (spin Hall effect) or temperature gradients (spin Nernst effect). We found that the transport properties of the considered systems are well approximated by Matthiessen's rule. In contrast to the longitudinal resistivities which are always underestimated, the Hall resistivities show positive and negative deviations from Matthiessen's rule. We demonstrate that the spin Hall and

spin Nernst conductivity of ternary alloys can be enhanced in comparison to the constituent binary alloys of equal total impurity concentration. This is not valid for the efficiency of the charge to spin current conversion described by the spin Hall angle. However, the efficiency of the heat to spin current conversion can be significantly enhanced in ternary alloys. For Cu(Bi_{0.75}Ti_{0.25}) it is increased by a factor of 4.5 in comparison to the Cu(Bi) alloy. This result offers a way for efficient spin current generation from temperature gradients in ternary alloys. In combination with Matthiessen's rule, this is a simple tool for material design of particular spintronics applications.

We thank N. F. Hinsche for helpful discussions. This work was supported by the Deutsche Forschungsgemeinschaft (DFG) via SFB 762 and the priority program SSP 1538. In addition, M.G. acknowledges financial support from the DFG via a research fellowship (GR3838/1-1).

*ktauber@mpi-halle.mpg.de

¹M. I. Dyakonov and V. Perel, *Phys. Lett. A* **35**, 459 (1971).

²J. E. Hirsch, *Phys. Rev. Lett.* **83**, 1834 (1999).

³Y. K. Kato, R. C. Myers, A. C. Gossard, and D. D. Awschalom, *Science* **306**, 1910 (2004).

⁴A. Fert, A. Friederich, and A. Hamzic, *J. Magn. Magn. Mater.* **24**, 231 (1981).

⁵T. Kimura, Y. Otani, T. Sato, S. Takahashi, and S. Maekawa, *Phys. Rev. Lett.* **98**, 156601 (2007).

⁶N. Nagaosa, J. Sinova, S. Onoda, A. H. MacDonald, and N. P. Ong, *Rev. Mod. Phys.* **82**, 1539 (2010).

⁷R. Karplus and J. Luttinger, *Phys. Rev.* **95**, 1154 (1954).

⁸J. Sinova, D. Culcer, Q. Niu, N. A. Sinitsyn, T. Jungwirth, and A. H. MacDonald, *Phys. Rev. Lett.* **92**, 126603 (2004).

⁹J. Smit, *Physica* **21**, 877 (1955).

¹⁰J. Smit, *Physica* **24**, 39 (1958).

¹¹L. Berger, *Phys. Rev. B* **2**, 4559 (1970).

¹²S. Lowitzer, M. Gradhand, D. Ködderitzsch, D. V. Fedorov, I. Mertig, and H. Ebert, *Phys. Rev. Lett.* **106**, 056601 (2011).

¹³Y. Niimi, M. Morota, D. H. Wei, C. Deranlot, M. Basletic, A. Hamzic, A. Fert, and Y. Otani, *Phys. Rev. Lett.* **106**, 126601 (2011).

¹⁴A. Fert and P. M. Levy, *Phys. Rev. Lett.* **106**, 157208 (2011).

¹⁵M. Gradhand, D. V. Fedorov, P. Zahn, and I. Mertig, *Phys. Rev. Lett.* **104**, 186403 (2010).

¹⁶M. Gradhand, D. V. Fedorov, P. Zahn, and I. Mertig, *Phys. Rev. B* **81**, 245109 (2010).

¹⁷Z. Ma, *Solid State Commun.* **150**, 510 (2010).

¹⁸X. Liu and X. Xie, *Solid State Commun.* **150**, 471 (2010).

¹⁹C. P. Chuu, M. C. Chang, and Q. Niu, *Solid State Commun.* **150**, 533 (2010).

²⁰K. Tauber, M. Gradhand, D. V. Fedorov, and I. Mertig, *Phys. Rev. Lett.* **109**, 026601 (2012).

²¹D. G. Rothe, E. M. Hankiewicz, B. Trauzettel, and M. Guigou, *Phys. Rev. B* **86**, 165434 (2012).

²²A. Dyrdał and J. Barnaś, *J. Phys.: Condens. Matter* **24**, 275302 (2012).

²³G. E. Bauer, A. H. MacDonald, and S. Maekawa, *Solid State Commun.* **150**, 459 (2010).

²⁴G. E. W. Bauer, E. Saitoh, and B. J. van Wees, *Nat. Mater.* **11**, 391 (2012).

²⁵Y. Niimi, Y. Kawanishi, D. H. Wei, C. Deranlot, H. X. Yang, M. Chshiev, T. Valet, A. Fert, and Y. Otani, *Phys. Rev. Lett.* **109**, 156602 (2012).

²⁶M. Gradhand, D. V. Fedorov, P. Zahn, I. Mertig, Y. Otani, Y. Niimi, L. Vila, and A. Fert, *Spin* **2**, 1250010 (2012).

²⁷M. Gradhand, M. Czerner, D. V. Fedorov, P. Zahn, B. Y. Yavorsky, L. Szunyogh, and I. Mertig, *Phys. Rev. B* **80**, 224413 (2009).

²⁸I. Mertig, *Rep. Prog. Phys.* **62**, 237 (1999).

²⁹I. Mertig, R. Zeller, and P. H. Dederichs, *Phys. Rev. B* **49**, 11767 (1994).

³⁰J. Ziman, *Electrons and Phonons* (Oxford University Press, Oxford, U.K., 2001).

³¹M. Gradhand, D. V. Fedorov, P. Zahn, and I. Mertig, *Solid State Phenom.* **168-169**, 27 (2011).

³²J. Ziman, *Principles of the Theory of Solids* (Cambridge University Press, Cambridge, U.K., 1964).